Available online at www.sciencedirect.com
SCIENCE DIRECT®
Journal of Nuclear Materials 353 (2006) 193–201
journal of nuclear materials
www.elsevier.com/locate/jnucmat

Surface mediated isotope exchange reactions between water and gaseous deuterium

Teboh F. Roland [a], Jacek Borysow [a,*], Manfred Fink [b]

[a] Department of Physics, Michigan Technological University, Houghton, MI 49931, USA
[b] Department of Physics, The University of Texas at Austin, Austin, TX 78712, USA

Received 6 July 2005; accepted 19 January 2006

Abstract

Maintaining isotopic purity of hydrogen is one of the major tasks in tritium processing systems. The work with multiple isotopes and isotopomers is accompanied by isotope exchanges which is often accelerated by catalysts e.g. surfaces of various materials. In this work, densities of D_2O, HDO produced via isotope exchange reactions in the mixture of D_2, H_2, D_2O, H_2O, HD and HDO contained in a stainless steel (type SS304) vessel were measured as a function of time (40–36 000 s) and pressures near 3.5×10^2 Pa, using mass spectrometry. The derived rates of change of the isotopomers densities are described accurately by a postulated kinetic model.

1. Introduction

One of the major issues in tritium processing systems is hydrogen isotopes identification and separation [1,2]. The formation of HD and TH molecules resulting from interactions between the material surface and the gaseous hydrogen isotopes mixtures of H_2, D_2 and T_2 has been the subject of many studies [3–6].

However, the database of actual rate coefficients of isotope exchange reactions at various materials is rather limited [7,8]. In this work we report rate coefficients for isotope exchange reactions between deuterium gas and water taking place at the surface of a stainless steel vessel.

2. Experiment

All experiments considered here were performed using the apparatus shown in Fig. 1. Each measurement involved four steps: (1) Surface cleaning; the reaction vessel was baked for several hours prior to every experiment. (2) Controlled surface adsorption of water (H_2O). (3) Isotopic exchange with molecular deuterium for different reaction times. (4) Measurement of surface desorption species using mass spectrometry.

The reaction vessel was built from standard 3.82 cm internal diameter conflat (CF) stainless steel (304 type) vacuum components. Copper gaskets were used between flanges. The specific volume of

* Corresponding author. Tel.: +1 906 370 5715.
E-mail address: jborysow@mtu.edu (J. Borysow).

0022-3115/$ - see front matter © 2006 Elsevier B.V. All rights reserved.
doi:10.1016/j.jnucmat.2006.01.018

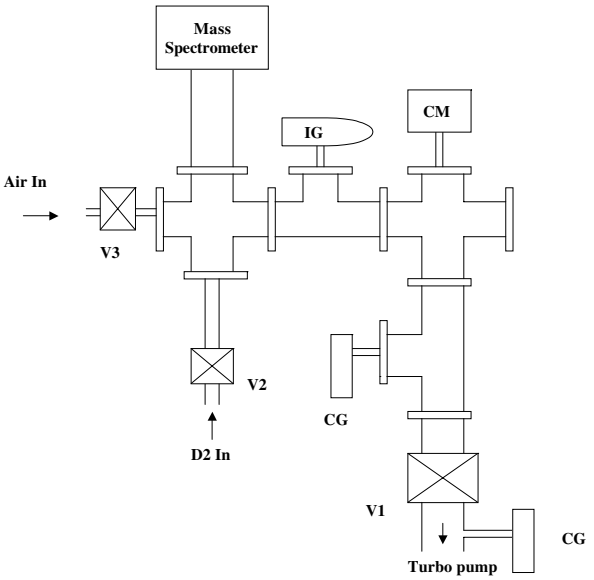

Fig. 1. Experimental setup: V_1, V_2, V_3 – manual valves, CM – capacitance manometer, CG – convectron pressure gauges, IG – ion pressure gauge. The whole reaction volume is made of standard CF stainless steel connected by copper gaskets.

the reaction vessel defined by the volume-to-surface ratio called σ is equal to 1.91×10^{-2} m. The system was baked for several hours before each experiment until the base pressure fell below 10^{-6} Pa. The system could be pumped down from 100 to 1.3×10^{-4} Pa by a 80 l/s turbo molecular pump in few seconds by opening valve V_1 in Fig. 1. The residual pressure was monitored by an ion gauge. The gasses were transferred into the reaction vessel through 0.64 cm internal diameter stainless steel tubing. The experiments were performed for various time durations (40–36 000 s) and pressures near 3.5×10^2 Pa. Capacitance manometer accurate to 1.3 Pa was used to monitor gas pressure. Two types of gasses were used in the measurements: deuterium with a purity of 99.5%, purified deuterium rated at 99.9%. The impurities were assumed to be H_2 and HD based on manufacturers specifications.

The water came from the laboratory air and the amounts were deduced from the measured relative humidity by a hygrometer accurate to ±5%. The number densities of the reactant gasses were measured by quadruple mass spectrometer with 1 atomic mass unit (amu) resolution. The mass spectrometer was calibrated to NIST traceable standards for most common gasses including all reactant gasses in our system. Its reading was accurate to ±10% on absolute scale in the range of pressures from 0.013 to 10^{-7} Pa.

2.1. Experimental methods

Prior to taking measurements the reaction vessel was baked out at a temperature of 250 °C for several hours, with valve V_1 opened until the system pressure reached mid 10^{-6} Pa. After baking, the residual pressure in the reaction vessel was recorded after the system returned to ambient temperature. Next, valve V_1 was closed and a measured quantity of moist laboratory air was introduced through valve V_3 into the vessel, typically 1.3×10^3 Pa. The procedures and experimental results of Shiraishi et al. [9] provided the tool to determine the amount of water vapor trapped on the vessel's walls. For a few seconds, valve V_1 was opened again and the nitrogen and oxygen of the original air were pumped from the reaction volume. During this time only a small amount of water was removed from the system as most of the water resides at the vessel walls. Next, valve V_1 was closed again and a few hundred Pa of D_2 was introduced into the reaction volume via valve V_2. This sets the beginning of the reaction time, t_R. Reaction times ranged from 40 s to 10 h. At the end of the reaction time, the valve V_1 was opened. It took about 3 s with valve V_1 opened until the pressure was sufficiently low for the mass spectrometer to record the partial pressures of the species present in the chamber. Most gaseous reaction species were pumped out at this time except for the water isotopomers adsorbed at the chamber walls. In all experiments reported here, water was never in a liquid phase [11]. A typical mass spectrum after a 40 s reaction time is shown

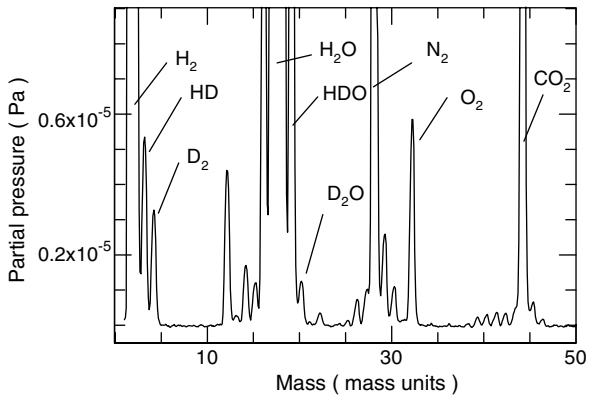

Fig. 2. Mass spectrum of the content of the reaction vessel after 40 s reaction time. The initial H_2O pressure was 2.0 Pa and D_2 pressure was 320 Pa. The spectrum was taken after evacuating the reaction vessel to pressure of 10^{-4} Pa.

in Fig. 2. The water and hydrogen isotopomers: HDO, HD, D_2O are clearly visible.

Two distinctive different reactions could potentially occur at the surface of the vessel walls: (1) Reactions between gasses introduced into the volume of the vessel with adsorbed water on the surface and then subsequently other isotopomers formed. (2) Reactions between the water isotopomers adsorbed at the vessel walls and the gasses evacuating from the wall material. These gasses have been trapped inside the vessel's walls sometime during the manufacturing process. The primary gas embedded in the stainless steel is atomic hydrogen [10]. The hydrogen diffuses to the wall where it recombines with another hydrogen atom residing already at the surface at a steady rate. The energy released during recombination is sufficient for the newly formed hydrogen molecule to desorb. Exchange reactions involving water isotopomers adsorbed at the wall and hydrogen also took place. The protium exiting the wall material can replace the deuterium in a deuterized water molecule and form HD, which will move from the surface into the vessel's volume. The protium's contribution to the reactants densities during the designated reaction time might be considered negligible as the number density of gasses introduced into the system were in the range of 10^4 larger than gasses released from the wall. When the measurements were taken, gasses leaving the walls were dominant after the reactants were pumped out and pressure dropped below 10^{-4} Pa. Therefore the number densities of HD, D_2, and H_2 could not be measured with our apparatus. It is an artifact that HD peak in Fig. 2 exceeds the D_2. D_2 peak is smaller than HD peak because gaseous deuterium was pumped out from the reaction vessel but HD was constantly produced by hydrogen atoms leaving the SS wall and reacting with water isotopomers adsorbed at the walls With this procedure it was impossible to differentiate between fraction of H_2 created during designated reaction time and the fraction formed at the wall in the outgassing process. Similar is true about HD, because some amounts of HD were produced by reactions of H_2 with adsorbed HDO and D_2O. The peaks corresponding to the hydrogen isotopes (H_2, HD, and D_2) in Fig. 2 do not reveal what took place during the designated reaction time, t_R. However, spectral lines in Fig. 2 provide reliable information about water isotopomers products. Based on results published by Shiraishi et al. [9] the amounts of water isotopomers residing on the walls of the reaction chamber were inferred from the outgassing rates. Shiraishi's [9] findings are summarized in Appendix I. In the following analysis it was assumed that in the sorption processes the mass transfer coefficients were the same for HDO, D_2O and H_2O. In order to measure an outgassing rate, the gasses and water were introduced to the reaction chamber and kept together for the time t_R, and then the valve V_1 was opened until most gas products were evacuated (usually for 3–5 s). After V_1 was closed and the partial pressures, for all water isotopomers were recorded as a function of time. The typical outgassing rates of all possible water isotopomers after 40 s reaction time are shown in Fig. 3. The conditions under which all experiments were performed are listed in Table 1.

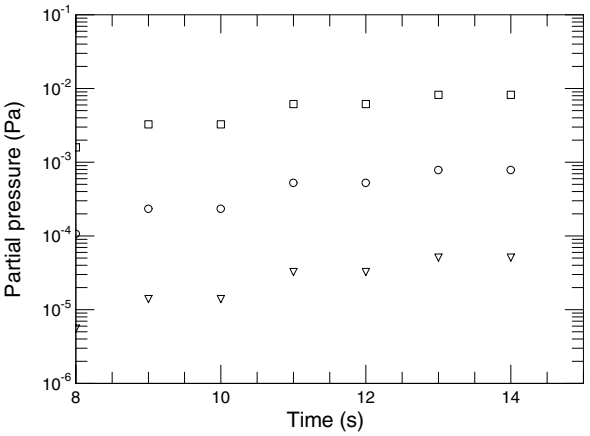

Fig. 3. The outgassing rates of water isotopomers after 40 s reaction time. The conditions are the same as in Fig. 2.

Table 1
List of the experiments performed

Experiments performed						
Time (s)	B.P. ($\times 10^{-6}$ Pa)	Temp. (K)	SVP (g/m^3)	RH (%)	Air in (Pa)	D_2 (Pa)
40	11	298.6	23.90	42	867	307
80	7.1	299.1	24.58	26	827	320
120	9.3	297.9	22.96	34	853	347
600	6.1	299.4	25.00	27	827	320
7200	10	298.6	23.90	36	920	333
18000	7.9	297.3	22.18	31	1130	333
36000	9.3	299.7	25.43	26	893	320

In column 2, BP is a base pressure (pressure measured by an ion gauge taken few seconds before experiment with main valve V_1 opened). SVP is the saturated vapor pressure in the laboratory air environment, which is the source of water in all experiments is listed in column 4. SVP was computed using semi-empirical formulas from references [16,17]. Column 5 gives relative humidity (RH) in the laboratory.

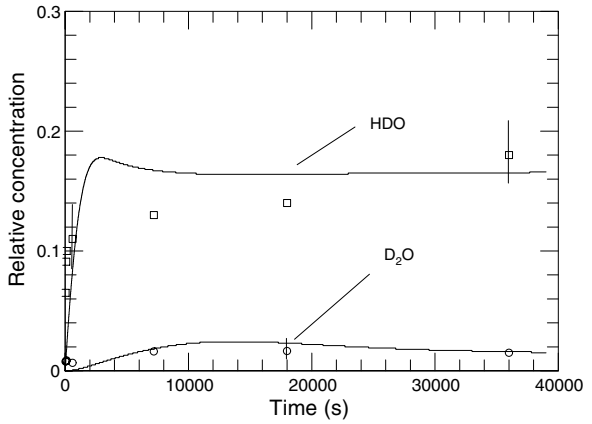

Fig. 4. The relative concentration of HDO (squares) and D_2O (circles) molecules as a function of time. The vertical lines illustrate typical reproducibility limits. The solid lines are result of the model calculations using the parameters k_i^0.

3. Results

The results are presented as relative concentrations or $HDO/(H_2O + HDO + D_2O)$ and $D_2O/(H_2O + HDO + D_2O)$ ratios for different time durations of the reaction. The ratios of reaction products as a function of time are shown in Fig. 4. Table 1 lists the conditions under which the subsequent experimental data points, shown in Fig. 4, were obtained. The relative concentrations of HDO as well as D_2O quickly reach steady state at about 15% and 2%, respectively. The vertical lines in Fig. 4 indicate experimental errors. These are maximum deviations or spread of values among repeated data runs. Typically three measurements were taken for similar initial conditions and the same reaction time. The initial conditions for each measurement were slightly different. Relative errors for short reaction times (±25%) are larger than for longer reaction times (±15%). The primary cause for the uncertainty was the time required to perform all the operations needed to take the experimental readings. The integrated time to fill the reactants and lower the pressure that a measurement can be done was about 15 s. The shortest reaction time attempted to measure the resulting isotopomers concentration was 40 s. The solid lines in Fig. 4 are the model calculations and are described next.

4. Kinetic model

The formation of HD, HDO, and D_2O molecules as a result of the interactions at the surface between D_2 and H_2O introduced into the reaction chamber is governed by isotopic exchange reactions. Ignoring higher order effects, the following reactions are possible:

$$H_2O + D_2 \overset{k_1}{\rightleftharpoons} HD + HDO, \quad (1)$$

$$D_2 + HDO \overset{k_2}{\rightleftharpoons} HD + D_2O, \quad (2)$$

$$H_2 + D_2O \overset{k_3}{\rightleftharpoons} HD + HDO, \quad (3)$$

$$H_2 + HDO \overset{k_4}{\rightleftharpoons} HD + H_2O, \quad (4)$$

$$H_2O + D_2O \overset{k_5}{\rightleftharpoons} 2HDO, \quad (5)$$

$$H_2 + D_2 \overset{k_6}{\rightleftharpoons} 2HD. \quad (6)$$

The equilibrium constants K_i for the reactions were calculated using statistical thermodynamics principles. Details about the computations are given in an Appendix II. The calculated equilibrium constants are listed in Table 2. The constant K_i is related to the forward and backward reaction rates by

$$K_i = \frac{k_i}{k_{-i}}, \quad (7)$$

where $i = 1, \ldots, 6$ corresponds to each of the six reactions and k_{-i} is used for the rate coefficient for the reverse reaction. The sixth reaction was ignored based on further analysis as it was unlikely to take place [12,13]. The only reactions of interest are therefore the ones catalyzed by the surface with water. The details of reactions kinetics are described in Appendix III.

4.1. Model predictions

At this time there is not enough independent experimental data to infer from time dependent measurements all rate coefficients in Eq. (13) in a unique form. Therefore, the numerical solutions of

Table 2
Molecular data used in the computations of equilibrium constants

Calculated K_i values		
Reactions ↓	K_i@298 K	$K_i(T)$ using $f(\text{vib}) \simeq 1$
$D_2 + H_2O \rightleftharpoons HD + HDO$	10.86	$3.12e^{371.84/T}$
$D_2 + HDO \rightleftharpoons HD + D_2O$	3.15	$0.74e^{432.01/T}$
$H_2 + D_2O \rightleftharpoons HD + HDO$	1.03	$5.72e^{-511.43/T}$
$H_2 + HDO \rightleftharpoons HD + H_2O$	0.30	$1.36e^{-451.26/T}$
$D_2O + H_2O \rightleftharpoons 2HDO$	3.43	$4.20e^{-60.17/T}$
$D_2 + H_2 \rightleftharpoons 2HD$	3.25	$4.24e^{-79.42/T}$

We follow notation from standard thermodynamics textbooks (e.g [15]).

postulated rate equations, Eq. (13), were fitted to the experimental data using nonlinear least squares routines.

4.1.1. Steady state solution

The time dependencies of HDO and D_2O shown in Fig. 4 suggest that the system reached the steady state. It was initially assumed, that the amount of hydrogen released from the walls during the reaction time is so small (about 4 orders of magnitude less than D_2) that it could be neglected. Following this assumption the H_2 outgassing rate α in Eq. (13) was set to zero. The steady state solution of the simplified model's (ignoring outgassing of hydrogen) was computed. In the experiment the initial mixture was 3.2×10^2 Pa, D_2 and 2.0 Pa of H_2O. The computed final partial pressures of the reactants in Eqs. (1)–(6) are: $P_{D_2} = 316$ Pa, $P_{HD} = 3.73$ Pa, $P_{H_2} = 0.0127$ Pa, $P_{D_2O} = 1.93$ Pa, $P_{H_2O} = 7.9\times10^{-5}$ Pa, $P_{HDO} = 0.124$ Pa. The steady state predictions obtained from simplified model were very much different than the measured results. Simplified model predicts that almost all water will be converted into D_2O and HDO. The computed relative concentrations HDO and D_2O were equal to 6.2×10^{-2} and 0.97, respectively, versus the experimental values of 0.15 and 0.02. Moreover, the simplified model predicted that in the steady state there will be about 15 times more D_2O than HDO, contradicting the experimental ratio of 0.13. Therefore the outgassing of hydrogen from the walls must be included in the model.

4.1.2. Numerical solution

The solid lines in Fig. 4 are the best fit of the kinetic model to the experimental points. In the fitting procedure, the rate coefficients $k_1,\ldots,k_5$ in Eq. (13) are free parameters. The initial conditions (amount of water, deuterium, HD) and outgassing rate of hydrogen α were taken from measurements.

First the rate equations (13) were solved numerically, using a computer code written within Fortran 90 standards with IMSL Library routine IVPRK [14]. Subroutine IVPRK solves an initial-value problem for ordinary differential equations using Runge–Kutta–Verner fifth-order and sixth-order method. The calculations give $D_2O(t)$, HDO(t), $H_2O(t)$, $D_2(t)$, HD(t), and $H_2(t)$ for a given set of rate coefficients and initial conditions.

Then a nonlinear least squares procedure using a modified Levenberg–Marquardt algorithm and a finite-difference Jacobian, provided by IMSL Library's UNLSF routine [14] was applied. The problem was posed as follows:

$$\min(k_1,\ldots,k_5)\frac{1}{2}\times\sum_{i=1}^{m}\left((D_2O(t_i))_{th}-(D_2O(t_i))_{exp}\right)^2+\left((HDO(t_i))_{th}-(HDO(t_i))_{exp}\right)^2, \quad (8)$$

where $(X)_{th}$ are computed (theoretical) values and $(X)_{exp}$ are experimental ones. All points have identical weighting factors.

The solution of the nonlinear least squares problem is: $k_1 = 3.29\times10^{-3}$ Pa^{-1} s^{-1}, $k_2 = 1.02\times10^{-3}$ Pa^{-1} s^{-1}, $k_3 = 4.59$ Pa^{-1} s^{-1}, $k_4 = 124$ Pa^{-1} s^{-1}, and $k_5 = 1.10\times10^{-2}$ Pa^{-1} s^{-1}.

We will refer to this set of rate equations as k_i^0 throughout the paper. The uniqueness of the above solution and the sensitivity of the model calculations on initial conditions was analyzed. Despite the fact that the model predicts the time transients for all six reactants the discussion is limited to water isotopomers as there is no reliable experimental data for gaseous species.

4.1.3. Model dependence on initial conditions

After finding the set of parameters $k_1,\ldots,k_5$ best describing the experimental data we computed time transients of reactants with different initial conditions. The initial D_2 number density was known with great precision (about 0.01%), however the determination of the amount of water in the reaction vessel was not straightforward and might carry a large error. The model results showed little change in computed time transients when we varied initial water concentration within factor of 2. This low sensitivity reflects the fact that the initial ratio of principal reactants D_2 to H_2O was very large (about 10^3) even after changing amounts of water by 100%. The computed reactants time transients without outgassing of hydrogen shown in Fig. 5 are also very different from the measured ones.

One other issue was the amount of HD in our deuterium reservoir. The computed relative partial concentration as a function of time of D_2O remained approximately the same when initial D_2/HD ratio was varied from 10^4 to 10^3 (see Fig. 6). The changes in the HDO time transient are very significant, in particular the initial build up of HDO. We made an attempt to verify the model predictions and made measurements of HDO buildup using

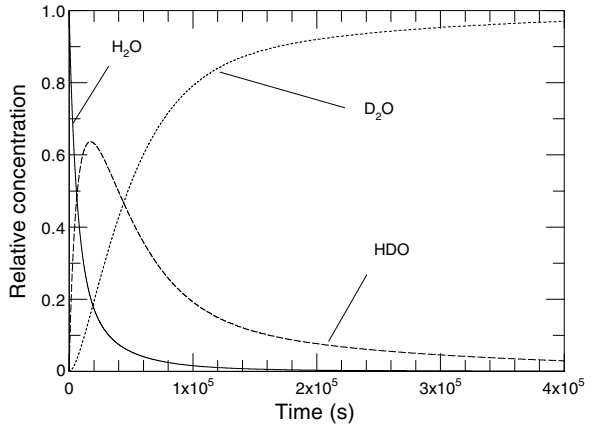

Fig. 5. Model predictions of the water isotopomers time transients with outgassing rate α set to zero with parameters k_i^0. The initial H_2O pressure was 2.0 Pa and D_2 pressure was 320 Pa.

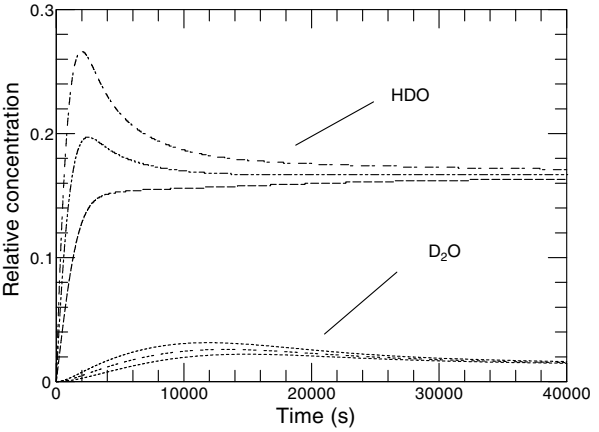

Fig. 6. The model calculations of the water isotopomers time transients with outgassing included for different initial partial pressure of HD. The HD concentration varied from 1.3×10^{-2} Pa (fastest initial HDO buildup) to 1.3×10^{-3} Pa (slowest HDO buildup). Other conditions like in Fig. 5.

purified deuterium, which contained 10 times less HD than in our standard experiments. The initial production of HDO was significantly slower (at least factor of 3). We were unable to make quantitative statements as we possessed only very small amounts of ultra pure D_2 and only a few experiments could be carried out. However, we feel confident to make the qualitative statement that water reactions with HD are much faster than with D_2.

4.1.4. Model dependence on parameters

In a multiparameter least square fit it is important to investigate which parameter is correlated with the quantity of interest. In all tests all parameters are kept fixed but one, which is varied within an order of magnitude. Our model appears to be fairly insensitive for manipulating parameters $k_3, \ldots, k_5$. Only small variations in the HDO and D_2O concentrations result from large changes in these parameters. This is caused by the small amounts of D_2O and therefore its overall contribution to the total amounts of reactants from e.g. reaction equation (5) is very small. Reactions Eqs. (3) and (4) described by k_3 and k_4 are very fast that the products are entirely controlled by the outgassing rate of H_2. The fact that k_3 and k_4 are orders of magnitude larger than the other rate coefficients does not mean that reaction of water isotopomers with H_2 are much faster. It simply accounts for reactions of atomic hydrogen leaving the walls and reacting with D_2O and HDO. The model is very sensitive to the k_1-coefficient which is responsible mostly for the production of HDO under our experimental conditions. Fig. 7, demonstrates how the steady state level of HDO depends on k_1-coefficient. It does not influence the buildup rate of HDO just its asymptotic amount. Finally, our model shows a similar high sensitivity to variations of the k_2-coefficient as far as the production of D_2O is concerned. Variations in the k_2-magnitude affects little the final HDO level but has a great influence on D_2O time transient (see Fig. 8).

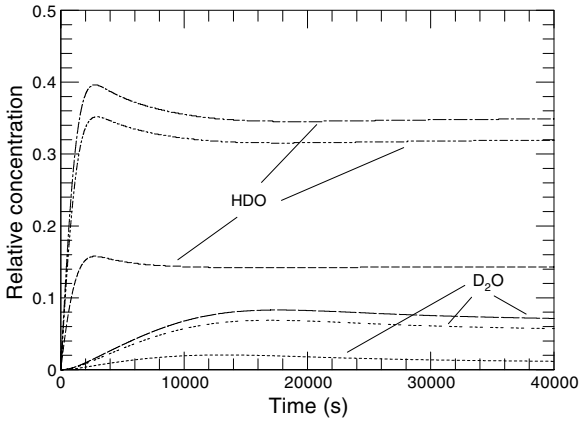

Fig. 7. Dependence of relative concentrations of HDO and D_2O computed for different rate coefficient k_1. All other coefficients are like in Fig. 5. The outgassing of hydrogen is included. The lowest concentrations resulted for $k_1 = 2.7 \times 10^{-3}\ \mathrm{Pa^{-1}\,s^{-1}}$, in between for $k_1 = 1.06 \times 10^{-2}\ \mathrm{Pa^{-1}\,s^{-1}}$ and highest $k_1 = 1.3 \times 10^{-2}\ \mathrm{Pa^{-1}\,s^{-1}}$.

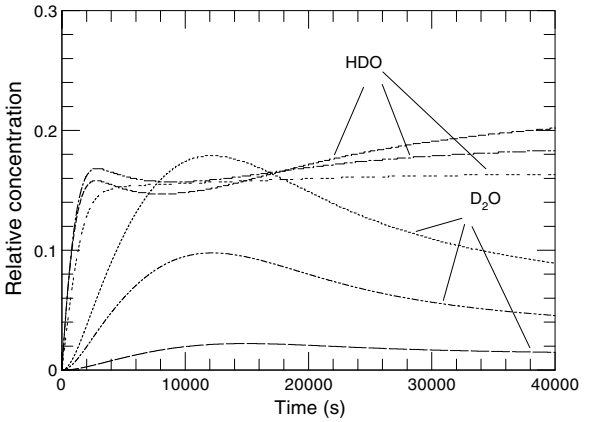

Fig. 8. Variations in the concentrations and time transients of D_2O and HDO shown for different rate coefficient k_2. The lowest concentration of D_2O was found for $k_2 = 1.02 \times 10^{-3}\,Pa^{-1}\,s^{-1}$, medium for $k_1 = 5.3 \times 10^{-3}\,Pa^{-1}\,s^{-1}$ and largest for $k_1 = 1.1 \times 10^{-2}\,Pa^{-1}\,s^{-1}$.

5. Conclusions

Time transients of D_2O and HDO produced via isotope exchange reactions in the mixture of D_2, H_2, D_2O, H_2O, HD and HDO contained in a stainless steel (type SS304) vessel were measured. The results were represented fairly well by the kinetic model in the form of coupled rate equations. The parameters of the model obtained and described in this paper can be used to predict the production of water isotopomers in similar systems. The validity of the model is limited to low pressure environment and large gas (D_2) to water ratios.

Acknowledgements

Support from NSF (PHY-0457194) and R.A. Welch Foundation at UT (F-1554) is gratefully acknowledged. At MTU financial assistance from Dean of College of Sciences and Arts and VP for research is much appreciated. Authors thank Katherine Cocciarelli for her linguistic help with the manuscript.

Appendix I

In order to deduce what fraction of the water vapor is trapped on the walls when a fixed amount of humid air is introduced into the chamber, the procedures and experimental results of Shiraishi et al. [9] were used. They have shown that the amount of water adsorbed on the walls of SS chamber can be determine by

$$q = 6.04 \times 10^{-6} P^{2/3}, \tag{9}$$

where, q (mol/m^2) is the amount of water adsorbed on the walls, and P (Pa) is the partial pressure of water introduced into the chamber.

In the same article Shiraishi et al. [9] have derived semi-empirical formulas relating outgassing rates of water to the amount of water residing on the chamber's surface. If the outgassing rate is measured in Pa/s, the partial pressure of water after all of it desorbs is given by

$$P_{H_2O} = \frac{\sigma}{k_F} \times OR_{H_2O}, \tag{10}$$

where, k_F is the mass transfer coefficient (MTC), OR_{H_2O} is the outgassing rate of H_2O, and σ is volume-to-surface ratio. If the MTC is the same for HDO as well as D_2O, the partial pressures for the latter species can be expressed as

$$\begin{aligned} P_{HDO} &= \frac{\sigma}{k_F} \times OR_{HDO}, \\ P_{D_2O} &= \frac{\sigma}{k_F} \times OR_{D_2O}, \end{aligned} \tag{11}$$

where, OR_{D_2O} and OR_{HDO} is the outgassing rate of D_2O and HDO, respectively. In all calculations we used value $k_F = 1.49 \times 10^{-3} \exp(-2.42 \times 10^3/RT)$ for stainless steel [9].

Appendix II

The equilibrium constants (K_i) for the reactions in Eqs. (1)–(6). were computed using thermodynamics principles. They are listed in Table 3. We used textbook of McQuarrie [15] as our reference. The constants listed in Table 1, compiled from the reference databases [11] were used in the calculations.

The fundamental vibrational frequencies are large in all of the cases so we assumed that exponential factors $[1 - \exp(-\Theta_v/T)]$ in the vibrational partition functions are essentially unity near room temperature. The temperature dependence of equilibrium constants as given in Table 2 are valid under such an assumption only.

Appendix III

The set of coupled differential equations below, describe all reactions taking place at the walls.

Table 3
Computed equilibrium constants for the reactions in Eqs. (1)–(6)

Table of molecular constants							
Species ↓	Molar mass	σ	$p \times 10^{120}$	Θ_r (K)	Θ_v (K)	v_j (cm^{-1})	H^0 (kJ mol^{-1})
H_2	2	2	–	85.4	6214.05	–	0
D_2	4	2	–	42.7	4394	–	0
HD	3	1	–	64.05	5381.53	–	0.33
H_2O	18	2	5.84	–	–	3657, 1595, 3756	−238.92
HDO	19	1	16.1	–	–	3707, 2727, 1402	−242.34
D_2O	20	2	40.4	–	–	2671, 1178, 2788	−246.26

$$\begin{aligned}\frac{dP_{HDO}}{dt} &= k_1\left(P_{D_2}P_{H_2O} - \frac{P_{HD}P_{HDO}}{K_1}\right)\\ &+ k_2\left(\frac{P_{HD}P_{D_2O}}{K_2} - P_{D_2}P_{HDO}\right)\\ &+ k_3\left(P_{H_2}P_{D_2O} - \frac{P_{HD}P_{HDO}}{K_3}\right)\\ &+ k_4\left(\frac{P_{HD}P_{H_2O}}{K_4} - P_{H_2}P_{HDO}\right)\\ &+ 2k_5\left(P_{H_2O}P_{D_2O} - \frac{P_{HDO}^2}{K_5}\right). \end{aligned} \quad (12)$$

In symbolic form

$$\begin{aligned}(P_{HDO})' &= \lambda_1 k_1 + \lambda_2 k_2 + \lambda_3 k_3 + \lambda_4 k_4 + 2\lambda_5 k_5,\\ (P_{HD})' &= \lambda_1 k_1 - \lambda_2 k_2 + \lambda_3 k_3 - \lambda_4 k_4,\\ (P_{D_2})' &= -\lambda_1 k_1 + \lambda_2 k_2,\\ (P_{H_2})' &= -\lambda_3 k_3 + \lambda_4 k_4 + \alpha t,\\ (P_{H_2O})' &= -\lambda_1 k_1 - \lambda_4 k_4 - \lambda_5 k_5,\\ (P_{D_2O})' &= -\lambda_2 k_2 - \lambda_3 k_3 - \lambda_5 k_5,\end{aligned} \quad (13)$$

where α is the measured outgassing rate of H_2 after the bake out of the system and is equal to 5.3×10^{-5} Pa/s, the coefficients λ_i are defined in Eq. (12) and $(P_X)'$ is a time derivative of the partial pressure. The rate equations describing the dynamics in our system are written in such form as if the reactions would take place in the gaseous phase. In reality most of the water is on the walls. The partial pressures in Eq. (13) are the equivalent pressures if all of the water would be in the volume of the reaction vessel and none would reside on its surface.

Only three equations in the postulated kinetic model equation (13) are linearly independent. These equations were obtained by row-echelon reduction of an augmented matrix. The other three, integrated with initial conditions produce mass conservation laws which are valid at all times. The total number of deuterium atoms, hydrogen atoms and oxygen atoms must remain unchanged and equal to numbers introduced at time equal zero into the reaction vessel

$$\begin{aligned}2 * P_{D_2} + P_{HD} + P_{HDO} + 2 * P_{D_2O} &= a,\\ 2 * P_{H_2} + P_{HD} + P_{HDO} + 2 * P_{H_2O} &= b + 2\alpha t,\\ P_{HDO} + P_{D_2O} + P_{H_2O} &= c,\end{aligned} \quad (14)$$

where a, b, and c are the number of deuterium, hydrogen atoms and water molecules respectively, introduced initially to the system. The set of coupled differential equations (13) can be solved simultaneously providing all rate coefficients k_i and outgassing rate α are known.

References

[1] Masabumi Nishikawa, Toshiharu Takeishi, Yoshinori Kawamura, Yuji Takagi, Yuzuru Matsumoto, Fus. Technol. 21 (1992).
[2] H.J. Kim, Y.D. Park, W.M. Lee, Plasma Chem. Plasma Process. 20 (2000) 2.
[3] D. Ducret, C. Laquerbe, A. Ballanger, J. Steimetz, V. Porri, J.P. Verdin, T. Pelletier, Fus. Sci. Technol. 41 (2002) 1092.
[4] A.A. Pisarev, P.O. Kokurin, Yu.V. Borisyuk, Tech. Phys. Lett. 24 (1998) 924.
[5] Kaname Kizu, Alexander Pisarev, Tetsuo Tanabe, J. Nucl. Mater. 289 (2001) 291.
[6] A. Zuttel, Ch. Nutzenadel, G. Schmid, Ch. Emmenegger, P. Sudan, L. Schlapbach, Appl. Surf. Sci. 162&163 (2000) 571.
[7] Nobuyuki Nakashio, Junya Yamaguchi, Ryusuke Kobayashi, Masabumi Nishikawa, Fus. Sci. Technol. 39 (2001) 2.
[8] I. Cristescu, U. Tamm, Ioana-R. Cristescu, M. Glugla, C.J. Caldwell-Nichols, Fus. Eng. Des. 61&62 (2002) 537.
[9] Tomofuni Shiraishi, Satoshi Odoi, Masabumi Nishikawa, Nucl. Sci. Technol. 34 (1997) 7.
[10] R.L. Paul, R.M. Lindstrom, J. Radioanal. Nucl. Chem. 243 (2000) 181.
[11] NIST databases, <http:srdata.nist.gov/cccbdb/default.htm>.
[12] G.T. McConville, D.A. Menke, R.E. Ellefson, J. Vac. Sci. Technol. A 1 (1983) 1441.
[13] J. Borysow, M. Fink, J. Nucl. Mater. 341 (2005) 224.

[14] User's Manual, IMSL Math/Library: FORTRAN subroutines for mathematical applications, IMSL – Problem-Solving Software Systems, 1989.
[15] Donald A. McQuarrie, Statistical Mechanics, University Science Books (2000).
[16] Website on Experimental Fit Data for Relative Humidity Calculation, <http:hyperphysics.phy-astr.gsu.edu/hbase/kinetic/relhum.html>.
[17] M.E. Jensen, R.D. Burman, R.G. Allen, ASCE Manuals and Reports on Engineering Practice No. 70, 1990.